Magnetic Control of Spin-Orbit Fields: A First-Principles Study of Fe/GaAs Junctions

Martin Gmitra,[1] Alex Matos-Abiague,[1] Claudia Draxl,[2] and Jaroslav Fabian[1]
[1]*Institute for Theoretical Physics, University of Regensburg, 93040 Regensburg, Germany*
[2]*Physics Department, Humboldt-Universität zu Berlin, 12489 Berlin, Germany*
(Received 22 February 2013; published 17 July 2013)

The microscopic structure of spin-orbit fields for the technologically important Fe/GaAs interface is uncovered from first principles. A symmetry based method allows us to obtain the spin-orbit fields—both their magnitude and orientation—for a generic Bloch state, from the electronic band structure for any in-plane magnetization orientation. It is demonstrated that the spin-orbit fields depend not only on the electric field across the interface, but also surprisingly strongly on the Fe magnetization orientation, opening prospects for their magnetic control. These results give important clues in searching for spin-orbit transport and optical phenomena in ferromagnet/nonmagnet heterostructures.

DOI: 10.1103/PhysRevLett.111.036603 PACS numbers: 72.25.Mk, 73.20.−r, 75.76.+j

In solid-state systems lacking space inversion symmetry, spin-orbit coupling (SOC) acts on the electronic structure as a spin-orbit field (SOF), which is an effective magnetic field whose direction and magnitude depend on the electron momentum [1,2]. The most prominent examples are the Dresselhaus spin-orbit field [3], describing the effects of bulk inversion asymmetry in zinc blende semiconductors, and the Bychkov-Rashba spin-orbit field [4], describing the effects of structure inversion asymmetry in asymmetric quantum wells. Apart from semiconductor structures, where Bychkov-Rashba coupling has been extensively studied [2,5,6], it has been investigated in many other systems, for example, on metallic surfaces [7–12], graphene on a Ni substrate [13], or in Au and Ag monolayers on W(110) substrates [14]. A striking manifestation of spin-orbit coupling in condensed matter is the spin-momentum locking in topological insulators [15].

Spin-orbit coupling can be controlled by an electric field [16]. This fact has long been used to motivate spintronics applications as epitomized by the Datta-Das transistor [17] in which the gate controls the spin-orbit induced spin precession of the itinerant electrons in a transistor channel. But spin-orbit coupling is also important for anisotropic magnetotransport. Tunneling anisotropic magnetoresistance (TAMR), for example, can be used to control electrical transport by rotating the magnetization orientation of a single ferromagnetic layer. It has been observed and studied in a variety of systems, GaMnAs/Al [18], Fe/GaAs, [2,19], CoFe/GaAs [20] (inserting a MgO barrier suppresses TAMR here [21], a clear evidence for interface induced symmetry of the effect), Co/Pt [22], Si/ferromagnet junctions [23], resonant tunnel devices [24], or on an atomic scale in STM experiments [25]. Interfacial spin-orbit coupling has been proposed to control thermoelectric anisotropies in helimagnetic tunnel junctions [26] and produce spin-transfer torque in ferromagnet-topological insulator junctions [27].

In earlier studies of spin-orbit coupling on surfaces [7–9,11,12,28] and interfaces [13,14], the spin-orbit Hamiltonian was extracted by fitting the energy bands close to the Γ point assuming a Bychkov-Rashba-type coupling. This standard procedure requires *a priori* knowledge of the specific functional form of the spin-orbit field and applies only to very small $\mathbf{k}$ vectors for which small-momentum expansions are meaningful. Here, we introduce a novel method to obtain spin-orbit fields (not just the functional parameters) for a generic $\mathbf{k}$ point directly from *ab inito* data. On the example of an Fe/GaAs junction, important for room temperature spin injection [29–33] and TAMR [19,34], we derive a formula for the magnitude and direction of the momentum dependent spin-orbit fields directly from the electronic band structure. The results show highly anisotropic (with respect to the momentum orientation) patterns, which take on different forms, from the ones known in semiconductor physics for small momenta to more exotic ones for Bloch states further away from the Γ point.

One fascinating outcome is a qualitative dependence of the spin-orbit field patterns on the band (energy), consistent with the bias-induced inversion of the TAMR observed in experiments [19,35]. Even more important, in addition to their sensitivity on an electric field, the spin-orbit fields can depend unusually strongly on the magnetization direction, to the point that the anisotropy axes can be flipped by rotating the magnetization. We emphasize that those effects are caused by the symmetry of the interface, not of the bulk structures, making them particularly important for lateral transport in ultrathin hybrid ferromagnet-nonmagnet junctions.

We consider thin Fe/GaAs slabs. The small lattice mismatch between twice the lattice constant of Fe (2.87 Å) and GaAs (5.65 Å) allows for a smooth epitaxial growth of Fe on a GaAs (001) surface. Early investigations of the stability of 1×1 Fe/GaAs interfaces within density functional theory [36] showed that, when more than two atomic layers

of Fe are deposited on a GaAs (001) surface, the flat or partially intermixed interfaces are more stable than the fully intermixed one, the As-terminated flat interface being more stable than the partially intermixed one. On the other hand, a recent Z-contrast scanning transmission electron microscopy reported a single plane of alternating Fe and As atoms at an Fe/AlGaAs interface [37,38]. Since the choice of the interface is not important to the message of our Letter, we choose an As-terminated flat interface.

The electronic structure of an ideal Fe/GaAs slab, containing 9 (001) atomic layers of GaAs with the diagonal lattice spacing $d = a/\sqrt{2} = 3.997$ Å and three atomic planes of bcc Fe has been calculated using the full potential linearized augmented plane wave technique implemented in the FLEUR code [39] and a generalized gradient approximation for the exchange-correlation functional [40]. The code uses the scalar relativistic approximation; the SOC for the valence electrons is treated within the second variational method.

The band structure of the Fe/GaAs slab along the high symmetry lines connecting the S-Γ-X points in the BZ is shown in Fig. 1 for a magnetization orientation along the $[1\bar{1}0]$ direction. The spin character of bands 1 and 2 in Fig. 1 is basically determined by the interface atoms. The interface unit cell contains interfacial As, the neighboring Ga, and two Fe atoms. The spin-up character of band $n = 2$ is dominated by the interfacial As atom, its neighboring Ga atom, and Fe atom above Ga, while the spin-down character of band $n = 1$ comes mostly from the two Fe atoms.

The noncentrosymmetric GaAs layer is of D_{2d} symmetry, exhibiting the bulk inversion asymmetry spin-orbit coupling. The interface lowers the symmetry to C_{2v} with the twofold rotation axis C_2 along the growth direction [001] [2]. The C_{2v} symmetry accounts for both the bulk inversion asymmetry and the structure inversion asymmetry; the C_{2v} spin-orbit field lies in the plane of the slab, perpendicular to the growth direction. Since C_{2v} symmetry

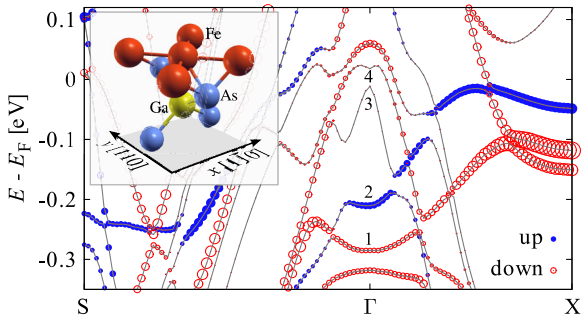

FIG. 1 (color online). Calculated band structure for the Fe/GaAs slab and magnetization along $[1\bar{1}0]$. The states with spin-up (spin-down) character at the Fe/GaAs interface are emphasized by blue filled (red open) circles whose radii are proportional to the corresponding charge density at the interface atoms. The inset shows the As-terminated flat 1×1 interface model assumed in the study.

has only one-dimensional orbital irreducible representations, away from accidental level (anti)crossings the spin-orbit fields (even at high symmetry points) can be described by spin-1/2 Pauli matrices.

The most general SOC Hamiltonian consistent with C_{2v} symmetry can be written for the in-plane momenta around the Γ point as

$$\mathcal{H}_{\rm so} = \mu_n(k_x, k_y, \varphi)k_x\sigma_y + \eta_n(k_x, k_y, \varphi)k_y\sigma_x, \quad (1)$$

where k_x and k_y are the components of the in-plane wave vector $\mathbf{k}$, σ_x and σ_y are the Pauli matrices, and x and y correspond to the diagonal $[1\bar{1}0]$ and [110] crystallographic directions in GaAs, respectively, φ refers to the magnetization direction with respect to the $[1\bar{1}0]$ crystallographic direction of GaAs, and n is the band index. The functional parameters μ_n and η_n,

$$\mu_n(k_x, k_y, \varphi) = \mu_n^{(0)}(\varphi) + \mu_n^{(1)}(\varphi)k_x^2 + \mu_n^{(2)}(\varphi)k_y^2 + \cdots,$$
$$\eta_n(k_x, k_y, \varphi) = \eta_n^{(0)}(\varphi) + \eta_n^{(1)}(\varphi)k_x^2 + \eta_n^{(2)}(\varphi)k_y^2 + \cdots, \quad (2)$$

are even in the momenta and, what is crucial and new here, depend in general on the magnetization direction. The out-of-plane SOFs vanish due to time reversal and structural C_{2v} symmetry.

The values of the expansion parameters $\mu_n^{(i)}$, $\eta_n^{(i)}$ ($i = 0, 1, 2, \ldots$) determine the specific form of the SOF. For example, if $\mu_n^{(0)} = \alpha_n$ and $\eta_n^{(0)} = -\alpha_n$ ($\mu_n^{(0)} = \eta_n^{(0)} = \beta_n$), $\mathcal{H}_{\rm so}$ reduces in the limit of small $k = |\mathbf{k}|$ to the well-known Bychkov-Rashba [4] (linearized Dresselhaus [3]) SOC with α_n (β_n) denoting the Bychkov-Rashba (Dresselhaus) SOC parameter of the nth band. By introducing the SOF,

$$\boldsymbol{w}_n(k_x, k_y, \varphi) = \begin{pmatrix} \eta_n(k_x, k_y, \varphi)k_y \\ \mu_n(k_x, k_y, \varphi)k_x \\ 0 \end{pmatrix}, \quad (3)$$

Eq. (1) can be rewritten as $\mathcal{H}_{\rm so} = \boldsymbol{w}_n(\mathbf{k}) \cdot \boldsymbol{\sigma}$, where $\boldsymbol{\sigma}$ is the vector of the Pauli matrices.

We focus on the analysis of the effective SOFs for in-plane magnetization directions. A detailed discussion for the case of magnetization perpendicular to the interface plane is provided in the Supplemental Material [41]. Unlike the intrinsic spin-orbit coupling coming from the fine structure of the atomic orbitals forming a solid, which can be of the order of 1 eV, the magnitudes of the spin splittings due to SOFs are small, typically 1–100 meV. In view of the exchange fields which are some eVs, the SOFs can be considered a perturbation; the electrons spins are quantized along with magnetization. Within first order perturbation theory, using symmetry, we find (see the Supplemental Material for the details [41]) the following relations,

$$w_{nx}(\mathbf{k},\varphi)=\sigma\left[\frac{\Delta E_n^{\mathrm{so}}(\mathbf{k},\varphi)+\Gamma_n^{\mathrm{so}}(\mathbf{k},\varphi)}{2\cos\varphi}\right] \tag{4}$$

and

$$w_{ny}(\mathbf{k},\varphi)=\sigma\left[\frac{\Delta E_n^{\mathrm{so}}(\mathbf{k},\varphi)-\Gamma_n^{\mathrm{so}}(\mathbf{k},\varphi)}{2\sin\varphi}\right], \tag{5}$$

where

$$\Delta E_n^{\mathrm{so}}(\mathbf{k},\varphi)=\frac{E_n(\mathbf{k},\varphi)-E_n(-\mathbf{k},\varphi)}{2}, \tag{6}$$

$$\Gamma_n^{\mathrm{so}}(\mathbf{k},\varphi)=\frac{E_n(-k_x,k_y,\varphi)-E_n(k_x,-k_y,\varphi)}{2}, \tag{7}$$

and σ refers to the spin character of the nth band, which is well defined away from anticrossings. The above relations allow us to extract the components of the SOF directly from the *ab initio* energy bands. In the particular cases of $\varphi\approx\pi/2$ and $\varphi\approx 0$ the numerators and denominators in Eqs. (4) and (5), respectively, vanish. In such cases the SOF is obtained by L'Hôpital's rule. The validity of Eqs. (4) and (5) is not restricted to the vicinity of the Γ point but holds also for large momenta. The only restriction is that the k-space region of interest must be away from energy anticrossings.

Figure 2 establishes the proof of principle for the magnetization dependence of SOFs. It shows the SOF, $\boldsymbol{w}(\mathbf{k})$ (bottom parts), and polar plots of its strength $w=|\boldsymbol{w}(\mathbf{k})|$ (upper parts), for the interface band $n=1$. The SOF is computed on three different contours around the Γ point, $k=\pi/100d$, $\pi/8d$, and $\pi/5d$ and is plotted in Figs. 2(a)–2(c), respectively. The left-hand (right-hand) panel corresponds to the magnetization pointing along $[1\bar{1}0]$ ([110]). The C_{2v} symmetry of the SOF is preserved for all k. In particular, close to the Γ point the SOFs resemble the interference of Bychkov-Rashba-type and Dresselhaus-type SOCs [see Fig. 2(a)]. However, away from the Γ point higher in k terms become relevant and more exotic patterns—we call them spin-orbit-field butterflies—in the SOF appear [see Figs. 2(b) and 2(c)]. The linear terms are dominant up to about 5% from the BZ center, where the SOF exhibits a very strong dependence on the magnetization orientation. Note that the principal symmetry axes of the SOF can even be flipped by turning the magnetization orientation. This remarkable effect opens the perspective of a magnetic control of spin-orbit fields.

Close to the Γ point the SOF is determined by the contributions linear in the wave vector components k_x and k_y and characterized by Bychkov-Rashba-type and Dresselhaus-type SOC parameters, $\alpha_n=[\mu_n^{(0)}-\eta_n^{(0)}]/2$ and $\beta_n=[\mu_n^{(0)}+\eta_n^{(0)}]/2$, respectively. Using Eqs. (2)–(6) we obtain (see Supplemental Material for more details [41])

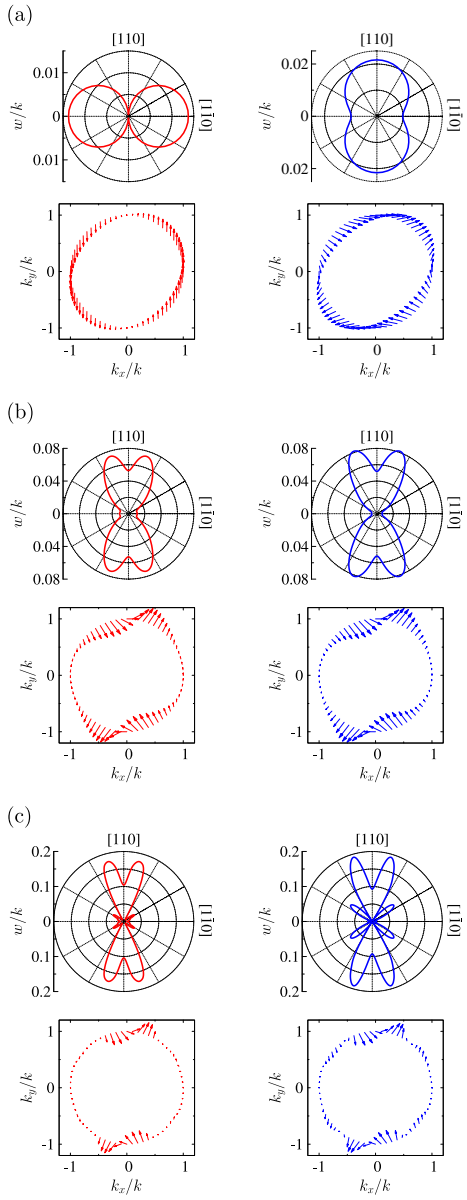

FIG. 2 (color online). Spin-orbit-field "butterflies." Calculated spin-orbit fields for the magnetization along $[1\bar{1}0]$ (left) and [110] (right). The polar plots of the spin-orbit coupling strength (w/k) in the units of eVÅ as well as the corresponding vector fields $\boldsymbol{w}(\mathbf{k})$ are shown for the band $n=1$ and the momentum contours of (a) $k=\pi/100d$, (b) $k=\pi/8d$, (c) $k=\pi/5d$. The lengths of the direction vectors have been rescaled.

$$\alpha_n(\varphi)=\sigma\left[\frac{a_n(\varphi)\cos\varphi-b_n(\varphi)\sin\varphi}{\sin(2\varphi)}\right] \tag{8}$$

and

$$\beta_n(\varphi)=\sigma\left[\frac{a_n(\varphi)\cos\varphi+b_n(\varphi)\sin\varphi}{\sin(2\varphi)}\right], \tag{9}$$

where $a_n(\varphi)=\partial E_n(\mathbf{k},\varphi)/\partial k_x|_{k=0}$ and $b_n(\varphi)=\partial E_n(\mathbf{k},\varphi)/\partial k_y|_{k=0}$. Thus, the dependence of $\alpha_n(\varphi)$ and

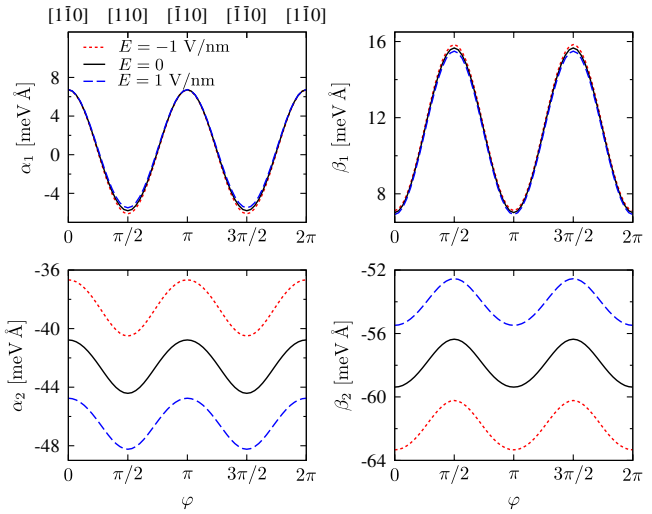

FIG. 3 (color online). Calculated magnetization and electric field dependence of the spin-orbit coupling parameters. The Bychkov-Rashba-type α_n and the Dresselhaus-type β_n spin-orbit parameters for the interface bands $n = 1, 2$ are shown as a function of the in-plane magnetization orientation and for different electric fields.

$\beta_n(\varphi)$ on the magnetization orientation can be obtained by computing the k-space gradient (velocity) of the *ab initio* energy bands in the vicinity of the Γ point. The functional forms of $a_n(\varphi)$ and $b_n(\varphi)$ conform to the symmetry requirements (see Supplemental Material [41]).

Figure 3 shows the magnetization dependence of the Bychkov-Rashba-type and Dresselhaus-type SOC parameters for the interface bands. The SOC parameters exhibit an oscillatory behavior as a function of the magnetization orientation. The angular dependence of the SOC parameters is stronger for band $n = 1$ than for $n = 2$. In particular, for the case of band $n = 1$ the Bychkov-Rashba-type SOC parameter can even change its sign when the magnetization is rotated in the plane. This leads to the sign change of the product $\alpha_1\beta_1$ when the magnetization is rotated from [1$\bar{1}$0] to [110] and produces the flipping of the SOF symmetry axes shown in Fig. 2(a). For band $n = 2$ the angular dependence is weaker, the product $\alpha_2\beta_2$ does not change its sign, and the symmetry axis of the SOF is preserved, being independent of the magnetization orientation.

When considering the dependence on the transverse electric field, the behavior is the opposite. Indeed, while the SOC parameters corresponding to band $n = 1$ change very little with E, for band $n = 2$ the changes in the magnitudes of α_2 and β_2 are appreciable. This disparate behavior is a consequence of the different nature of these two bands. Band $n = 1$ originates mostly from the two Fe atoms in the interface unit cell and, therefore, its corresponding SOF is more sensitive to the changes in the magnetization direction. However, the electrostatic control of the SOC parameters is dominated by the electric field influence on the pd bonding between As and Fe atoms.

TABLE I. Band-resolved expansion coefficients of the Bychkov-Rashba-type and Dresselhaus-type spin-orbit coupling parameters in meVÅ units. The parameters are in the range of what is found in semiconductors [2].

n	$A_n^{(+)}$	$B_n^{(+)}$	$A_n^{(-)}$	$B_n^{(-)}$
1	−0.42	−6.26	−11.32	4.32
2	−42.51	1.82	−57.94	−1.51
3	−620.24	−88.74	−597.56	−89.62
4	680.09	95.61	697.58	103.15

Consequently, the SOF corresponding to band $n = 2$, which comes mostly from the interfacial As atom, its neighboring Ga, and the Fe atom above Ga, exhibits a stronger dependence on the electric field.

In Table I we list the expansion coefficients of the SOC parameters (see Eqs. (23) and (24) in the Supplemental Material [41]),

$$\alpha_n \simeq A_n^{(+)} + B_n^{(+)} \cos(2\varphi), \tag{10}$$

$$\beta_n \simeq A_n^{(-)} + B_n^{(-)} \cos(2\varphi), \tag{11}$$

for zero electric field. From $A_n^{(+/-)}$ one extracts the magnetization-independent part, whereas the $B_n^{(+/-)}$ parameters control the leading contribution (higher order coefficients are about 2 orders smaller) to the angular (magnetization orientation) dependence of the spin-orbit parameters. In addition to the interface bands ($n = 1, 2$), we have also included the expansion coefficients corresponding to the As-surface bands ($n = 3, 4$), which, due to their surface nature, possess stronger SOFs.

To conclude, we introduced a method to obtain spin-orbit fields from first-principles or experimental band structures, going beyond the usually studied linear Rashba regime and providing a tool for realistic phenomenological modeling of spin-orbit effects. Although we used an important example of Fe/GaAs, our method is applicable to a broad class of ferromagnetic materials structures. Moreover, we found that the spin-orbit fields (and not only the band structure) depend strongly on the magnetization orientation. This shows that in order to realistically model spin-orbit effects in ferromagnetic heterostructures, say, with a tight-binding technique (which would also capture anticrossings not covered in our single-band method), one needs to consider the magnetoanisotropy of phenomenological fitting parameters. The magnetic control of SOFs may have important consequences for our understanding of and for predicting new spin-orbit phenomena in solids. In particular, lateral transport through a few monolayers of a ferromagnetic metal on a semiconductor could be strongly influenced by the interfacial spin-orbit fields of the kind reported here. One could also envisage spintronic device concepts based on spin-orbit fields and their magnetic

control, in analogy to their existing counterparts controlled electrically.

We thank D. Weiss, G. Bayreuther, C. Back, and G. Woltersdorf for useful hints related to experimental ramifications of the presented theoretical concepts and F. Freimuth, Y. Mokrousov, G. Bihlmayer, J. Spitaler, and P. Novák for helpful discussions regarding the calculations. This work has been supported by DFG SFB 689.

[1] I. Žutić, J. Fabian, and S. Das Sarma, Rev. Mod. Phys. **76**, 323 (2004).
[2] J. Fabian, A. Matos-Abiague, C. Ertler, P. Stano, and I. Žutić, Acta Phys. Slovaca **57**, 565 (2007).
[3] G. Dresselhaus, Phys. Rev. **100**, 580 (1955).
[4] Y. A. Bychkov and E. I. Rashba, JETP Lett. **39**, 78 (1984).
[5] R. Winkler, *Spin-Orbit Coupling Effects in Two-Dimensional Electron and Hole Systems* (Springer, Berlin, 2003).
[6] X. Cartoixá, L. W. Wang, D. Z.-Y. Ting, and Y. C. Chang, Phys. Rev. B **73**, 205341 (2006).
[7] S. LaShell, B. A. McDougall, and E. Jensen, Phys. Rev. Lett. **77**, 3419 (1996).
[8] J. Henk, A. Ernst, and P. Bruno, Phys. Rev. B **68**, 165416 (2003).
[9] Y. M. Koroteev, G. Bihlmayer, J. E. Gayone, E. V. Chulkov, S. Blügel, P. M. Echenique, and P. Hofmann, Phys. Rev. Lett. **93**, 046403 (2004).
[10] B. Fluegel, S. Francoeur, A. Mascarenhas, S. Tixier, E. C. Young, and T. Tiedje, Phys. Rev. Lett. **97**, 067205 (2006).
[11] C. R. Ast, J. Henk, A. Ernst, L. Moreschini, M. C. Falub, D. Pacilé, P. Bruno, K. Kern, and M. Grioni, Phys. Rev. Lett. **98**, 186807 (2007).
[12] F. Meier, H. Dil, J. Lobo-Checa, L. Patthey, and J. Osterwalder, Phys. Rev. B **77**, 165431 (2008).
[13] Y. S. Dedkov, M. Fonin, U. Rüdiger, and C. Laubschat, Phys. Rev. Lett. **100**, 107602 (2008).
[14] A. M. Shikin, A. Varykhalov, G. V. Prudnikova, D. Usachev, V. K. Adamchuk, Y. Yamada, J. Riley, and O. Rader, Phys. Rev. Lett. **100**, 057601 (2008).
[15] M. Z. Hasan and C. L. Kane, Rev. Mod. Phys. **82**, 3045 (2010).
[16] J. Nitta, T. Akazaki, H. Takayanagi, and T. Enoki, Phys. Rev. Lett. **78**, 1335 (1997).
[17] S. Datta and B. Das, Appl. Phys. Lett. **56**, 665 (1990).
[18] C. Gould, C. Rüster, T. Jungwirth, E. Girgis, G. M. Schott, R. Giraud, K. Brunner, G. Schmidt, and L. W. Molenkamp, Phys. Rev. Lett. **93**, 117203 (2004).
[19] J. Moser, A. Matos-Abiague, D. Schuh, W. Wegscheider, J. Fabian, and D. Weiss, Phys. Rev. Lett. **99**, 056601 (2007).
[20] T. Uemura, M. Harada, K. Matsuda, and M. Yamamoto, Appl. Phys. Lett. **96**, 252106 (2010).
[21] T. Akiho, T. Uemura, M. Harada, K. Matsuda, and M. Yamamoto, Appl. Phys. Lett. **98**, 232109 (2011).
[22] B. G. Park, J. Wunderlich, D. A. Williams, S. J. Joo, K. Y. Jung, K. H. Shin, K. Olejnik, A. B. Shick, and T. Jungwirth, Phys. Rev. Lett. **100**, 087204 (2008).
[23] S. Sharma, S. P. Dash, H. Saito, S. Yuasa, B. J. van Wees, and R. Jansen, Phys. Rev. B **86**, 165308 (2012).
[24] M. Tran, J. Peiro, H. Jaffres, J.-M. George, O. Mauguin, L. Largeau, and A. Lemaitre, Appl. Phys. Lett. **95**, 172101 (2009).
[25] K. von Bergmann, M. Menzel, D. Serrate, Y. Yoshida, S. Schröder, P. Ferriani, A. Kubetzka, R. Wiesendanger, and S. Heinze, Phys. Rev. B **86**, 134422 (2012).
[26] C. Jia and J. Berakdar, Appl. Phys. Lett. **98**, 192111 (2011).
[27] F. Mahfouzi, N. Nagaosa, and B. K. Nikolic, Phys. Rev. Lett. **109**, 166602 (2012).
[28] O. Krupin, G. Bihlmayer, K. Starke, S. Gorovikov, J. E. Prieto, K. Döbrich, S. Blügel, and G. Kaindl, Phys. Rev. B **71**, 201403 (2005).
[29] A. T. Hanbicki, B. T. Jonker, G. Itskos, G. Kioseoglou, and A. Petrou, Appl. Phys. Lett. **80**, 1240 (2002).
[30] S. A. Crooker, M. Furis, X. Lou, C. Adelmann, D. L. Smith, C. J. Palmstrøm, and P. A. Crowell, Science **309**, 2191 (2005).
[31] P. Kotissek, M. Bailleul, M. Sperl, A. Spitzer, D. Schuh, W. Wegscheider, C. H. Back, and G. Bayreuther, Nat. Phys. **3**, 872 (2007).
[32] P. Mavropoulos, O. Wunnicke, and P. H. Dederichs, Phys. Rev. B **66**, 024416 (2002).
[33] A. Perlov, V. Popescu, and H. Ebert, Phys. Status Solidi B **241**, 1316 (2004).
[34] R. Sykora and I. Turek, J. Phys. Condens. Matter **24**, 365801 (2012).
[35] A. Matos-Abiague and J. Fabian, Phys. Rev. B **79**, 155303 (2009).
[36] S. C. Erwin, S. H. Lee, and M. Scheffler, Phys. Rev. B **65**, 205422 (2002).
[37] T. J. Zega, A. T. Hanbicki, S. C. Erwin, I. Žutić, G. Kioseoglou, C. H. Li, B. T. Jonker, and R. M. Stroud, Phys. Rev. Lett. **96**, 196101 (2006).
[38] L. R. Fleet, H. Kobayashi, Y. Ohno, J. Y. Kim, C. H. W. Barnes, and A. Hirohata, J. Appl. Phys. **109**, 07C504 (2011).
[39] http://www.flapw.de/.
[40] J. P. Perdew, K. Burke, and M. Ernzerhof, Phys. Rev. Lett. **77**, 3865 (1996).
[41] See Supplemental Material at http://link.aps.org/supplemental/10.1103/PhysRevLett.111.036603 for details of general theory to obtain spin-orbit fields in case of in-plane and out-of-plane magnetization.